Article:
Panakoulia, S.K., Nikolaidis, N.P., Paranychianakis, N.V. et al. (2017) Factors Controlling Soil Structure Dynamics and Carbon Sequestration Across Different Climatic and Lithological Conditions. Advances in Agronomy, 142. pp. 241-276. ISSN: 0065-2113

https://doi.org/10.1016/bs.agron.2016.10.008

Factors controlling soil structure dynamics and carbon sequestration across different climatic and lithological conditions

Panakoulia S.K.*[,1], Nikolaidis N.P*., Paranychianakis N.V.*, Menon M.[†], Schiefer J.[§], Lair G.J.[§], Kram P.[¶], Banwart S.A.[r],

*School of Environmental Engineering, Technical University of Crete (TUC), University Campus, Chania, 73100, Greece An overview of APSIM, a model designed for farming systems simulation, in: European Journal of Agronomy

[†] Department of Geography, Winter Street, University of Sheffield, Sheffield S102TN United Kingdom

[r] School of Earth and Environment, University of Leeds, Leeds LS2 9JT, United Kingdom

[§] University of Natural Resources and Life Sciences (BOKU), Vienna, Peter-Jordan-Street 82, 1190 Vienna, Austria

[¶] Czech Geological Survey, Klarov 3, 118 21 Prague 1, Czech Republic

[1] Corresponding author: e-mail address: spanakoulia@gmail.com

Abstract

Soil organic carbon (SOC) is a strong determinant of soil fertility through its positive effects on soil structure and soil chemical and biological properties which in turn stimulate primary production. The objective of this work was to simulate field sites that represent different land uses and management practices in three continents, in order to identify the most important factors controlling soil structure dynamics and C sequestration across different climatic and lithological conditions as well as to quantify the rates of the afore-mentioned processes. The Carbon, Aggregation and Structure Turnover (CAST) model was used to simulate SOC sequestration, aggregate formation, and structure dynamics in three field sites including non tilled soils of natural ecosystems and tilled soils of agricultural fields in Europe (Critical Zone Observatories (CZO) of the SoilTrEC network) and one site in North America. Derived data from the simulations results, of SOC stocks and Water Stable Aggregate (WSA) particle size distribution, together with the respective results of three additional sites (Damma Glacier CZO, Milia (Greece) and Heilongjiang Mollisols (China)) were statistically analyzed in order to determine the factors affecting SOC sequestration and soil structure development. The natural

ecosystems include non tilled soils covered with natural local vegetation while the agricultural sites include cultivated and tilled soils covered with crops. The natural ecosystems were represented by Damma Glacier CZO (Switzerland), Heilongjiang Mollisols (China), Koiliaris CZO (Greece), Clear Creek (USA) and the Slavkov Forrest CZO (Czech Republic) whereas the agricultural field sites were located at Heilongjiang Mollisols (China), Koiliaris CZO (Greece), Clear Creek (USA), Marchfeld CZO (Austria) and Milia (Greece). Principal Component Analysis (PCA) identified clay content, bulk density, climatic conditions (precipitation and evapotranspiration), organic matter (OM) and its decomposition rates, as the most important factors that controlled soil structure development. The relative importance of each of these factors differs under differing climatic and lithological conditions and differing stages of soil development. Overall, the modeling results for both natural ecosystems and agricultural fields were consistent with the field data. The model reliably simulated C and soil structure dynamics in various land uses, climatic conditions and soil properties providing support for the underlying conceptual and mathematical modeling and evidence that the CAST model is a reliable tool to interpret soil structure formation processes and to aid the design of sustainable soil management practices.

Keywords: CAST model, soil structure, soil carbon, modeling

1. Introduction

1.1 Soil threats

The adoption of intense agricultural management practices, deforestation and livestock grazing has accelerated soil losses exceeding these of formation by approximately two orders of magnitude (Brantley et al., 2007) with important consequences for the role of soil in vegetation productivity worldwide (CEC, 2006). The EU as part of the 2006 Environment Policy Review previously published the Thematic Strategy for Soil Protection (CEC, 2006) as one of 7 thematic priorities. On 1 January 2016, the 17 Sustainable Development Goals (SDGs) of the 2030 Agenda for Sustainable Development, adopted by world leaders in September 2015, officially came into force. One of the “17 Goals to transform our World” by the United Nations, aims to protect, restore and promote sustainable

use of terrestrial ecosystems, sustainably manage forests, combat desertification, and halt and reverse land degradation and halt biodiversity loss (General Assembly, United Nations, 2015). Forests provide shelter to more than 80 per cent of all terrestrial species, 2.6 billion people depend directly on agriculture while 12 million hectares are lost every year due to drought and desertification, where 20 million tons of grain could have been grown. Over 80 per cent of the human diet is provided by plants and 60 per cent of the energy intake is provided only by three cereals. As a result 74 per cent of the poor are directly affected by land degradation (General Assembly, United Nations, 2015). Despite its critical role in the sustenance of the biosphere and meeting the food requirements of more than 7 billion global inhabitants, our knowledge of the soil functions and their response to human activity is far from complete. Thus, a great challenge in the soil science is to improve our understanding of soil processes, particularly for the critical soil functions as they are defined by EU Soil Thematic Strategy, and to develop suitable tools that will allow us to simulate and quantitatively evaluate the impacts of currently applied management practices, the potential impacts of future management practices, or the shifts in environmental conditions including changing land use and climate.

1.2 Soil Organic matter and fertility

Soil fertility strongly depends on soil organic matter (SOM) (Lal, 2015, 2004; Tiessen et al., 1994) by improving soil physical, chemical and biological properties that support primary production by vegetation. The formation of WSA favors the sequestration of C in the soils by protecting it from decomposition (Tisdall and Oades, 1982), reducing in this way CO_2 emissions to the atmosphere (Lal, 2004). The distribution of aggregates between the different size classes has been related to soil structure, SOM and biological activity and represents soil's ability to resist disintegration by disruptive forces (Six et al., 2000). The formation of WSA due to OM addition, improves soil structure and the hydraulic properties of bulk soil through the formation of larger connected pores resulting in increased bulk permeability to fluid flow and improved drainage, while increasing the water holding capacity within the microscopic pores of the larger aggregates. WSA formation is directly related to protection of SOM. SOM can chemically bind to soil mineral particles, making SOM less bioavailable in sorbed form, and also altering the surface properties of soil mineral to

favour particle-particle binding and aggregation (Nikolaidis and Bidoglio, 2013). Formation of larger aggregates also provides a redox barrier by holding water within the microscopic pores of the aggregates, which creates a diffusion barrier to O2 and protects the SOM against oxidative microbial degradation. On the other hand, soil structure is affected adversely by the mechanical shearing created by tillage, by freezing and thawing that results from extreme temperature fluctuations, and by the compaction that is due to the use of heavy machinery (Ross et al., 2015).

Restoration of soil fertility through soil management can be achieved by applying appropriate agro-ecological practices (Lal, 2013). Crop rotation, organic-C addition as SOM with associated nutrient elements, reduced tillage, use of cover crops during fallow periods, and controlled grazing are among the most commonly applied practices for sustainable agriculture (Milne et al., 2015). Incorporation of plant residues and organic amendments, such as compost and manure, combined with reduced tilling, enhance C sequestration (Lal, 2015) and plant production (Li et al., 2016; Liao et al., 2015) as well as soil hydraulic properties (hydraulic conductivity, water holding capacity, aeration, and porosity) (Udom et al., 2016). Field experiments with organic amendments have shown that manure improves soil structure and protection of aggregate-associated SOM much more than plant compost in terms of aggregate size and C content (Udom et al., 2016) while evidence has been provided that a mixture of compost (e.g. municipal solid waste derived) and manure (of a rate 70/30 respectively) is equally beneficial, resulting in the increase of the large (>250 μm) WSA mass fraction (Kotronakis et al., 2016; Udom et al., 2016). The effectiveness of these practices depends strongly on OM application rate and composition, climate, and other management practices.

1.3 Modeling soil carbon and structure dynamics

Mathematical models have been developed to simulate and predict soil structure development and C sequestration. These soil properties, as measured by WSA and soil C stocks and their rates of formation, provide proxy measures for soil fertility, defined here as the capacity of soil to support the rate of primary production by vegetation (e.g. g C fixed y^{-1} kg soil $^{-1}$). Over the past decades, several mathematical models were developed to simulate SOC dynamics. Mathematical models such as

CENTURY (Parton et al., 1987), Roth-C (Coleman, K., Jenkinson, 1999; Jenkinson, 1990), DNDC (Gilhespy et al., 2014; Li et al., 2005) and APSIM (Keating et al., 2003), have been used (Álvaro-Fuentes and Paustian, 2010; Andrianaki et al., 2016; Carvalho Leite et al., 2004; Dou et al., 2014; Galdos et al., 2009; GAO et al., 2008; Goglio et al., 2014; Luo et al., 2013; Poeplau and Don, 2015; Stamati et al., 2013b; Zhang et al., 2016) to assess the impact of land management on SOM stocks and to investigate the ability of these models to simulate long term (decades – centuries) SOM dynamics across different ecosystems (Smith et al., 1997). However, these models do not consider the effect of structure and its feedbacks on organic-C dynamics. Several studies have revealed a strong effect of structure on SOC turnover (Jastrow et al., 2007), identifying the link between OM decomposition and aggregate stability (Abiven et al., 2009), and summarizing the dynamics of SOC turnover with changes in soil structure (Nikolaidis and Bidoglio, 2013),. Existing models have been updated (Coleman and Jenkinson, 1999) or further modified (Jenkinson and Coleman, 2008; Nadeu et al., 2015), to incorporate the contribution of factors affecting SOC dynamics and aggregate formation. Over the last decade new models have been developed, and new conceptual frameworks on modeling of soil functions have been proposed. Abiven et al. (2008) developed the Pouloud model to predict the impact of organic residues incorporation on aggregate stability, under field conditions. The Struc-C model (Malamoud et al. 2009) was based on the RothC-26.3 model and linked SOM dynamics with soil aggregation and soil structure. The InVEST model (Nelson et al., 2009) was structured to predict changes in ecosystem services under different land use/land cover change scenarios, incorporating sub-routines assessing water service, soil conservation, C sequestration, biodiversity conservation and commodity production value. The SoilGen2 model (Finke, 2012), which is a further development of the SoilGen1 model (Finke and Hutson, 2008), is a 1D model that simulates the pedogenesis of various parent materials and includes clay formation, and has been used to successfully simulate soil formation. Segoli et al., (2013) developed the AggModel which is a combination of an aggregate dynamics model and a SOM dynamics model, where the C pools are not conceptual but directly measured. Finally, (Stamati et al., 2013a) developed the CAST model using an aggregation mechanism similar to the Struc-C model approach and modeling the carbon sequestration and turnover rates in each aggregate size.

136 The objective of this work is to use the results of the CAST model simulations of SOC and WSA
137 dynamics for 7 sites around the world with different land use management practices, including natural
138 and agricultural ecosystems, in order to characterize the process rates and the factors controlling soil
139 structure dynamics and C sequestration across different climatic and lithological conditions. A meta-
140 modeling Principal Component Analysis (PCA) integrates the results, clusters the sites by dominant
141 factors influencing SOC and structure dynamics, and identifies the principal factors controlling C
142 sequestration within the clustered sites.

143 2. Methodology and methods

144 The CAST model (Stamati et al., 2013a) was used to simulate soil structure dynamics and C
145 sequestration in seven sites across the world. The sites were the Koiliaris CZO, Slavkov Forest CZO,
146 Marchfeld CZO, Clear Creek (Iowa, USA), Damma Glacier CZO, Heilongjiang Mollisols (China) and
147 Milia (Greece), representing various climates, land management practices, soil properties and
148 histories. Table 1 presents the list of the natural ecosystems and agricultural fields of each study site.

149 [Insert Table 1 here]

150 The simulations of the CAST model from the Marchfeld CZO, Slavkov Forest CZO, and the
151 agricultural fields of Koiliaris CZO and Clear Creek are presented, while the simulations of Damma
152 Glacier CZO, Heilongjiang Mollisols, Milia and the natural ecosystems of Koiliaris CZO and Clear
153 Creek are described previously (Andrianaki, 2016; Li et al., 2016; Stamati et al., 2013a; Vavlas et al.,
154 2014). The geographic distribution of the sites evaluated in this work is shown in Figure 1.

155 [Insert Figure 1 here]

156 All model simulations were performed using consistent guidelines. The simulations were compared in
157 terms of the stocks and flows of C taking into account C sequestration, microbial biomass and the
158 CO_2 flux as well as the changes in the mass distribution of WSA size classes. A comparison of the
159 sites was conducted regarding the rate constants related to the processes of plant biomass
160 fragmentation, formation of micro- and macro-aggregates, SOC decomposition and aggregate

disruption. Finally, principal component analysis (PCA) was performed in order to identify the most significant model input, output and calibration parameters as the factors controlling SOC and soil structure dynamics and to identify sites across climatic and lithological gradients with similar responses to SOC sequestration. The model parameters that were included in the PCA analysis were selected based on a parameter sensitivity analysis conducted during the calibration process. The most sensitive (i.e. affecting the simulation results) input, output and model parameters were included in the PCA analysis. The PCA was performed using the MiniTab 17 statistical software.

Methods

2.1 Model Description

The CAST model simulates the mechanisms of aggregation assuming three size classes of aggregates: the silt-clay sized aggregates (AC1, < 53 μm), the micro-aggregates (AC2; 53-250 μm) and the macro-aggregates (AC3, > 250 μm). Figure 2 presents a schematic representation of the concept of WSA formation modified from Stamati et al. (2013). The model assumes that macro-aggregates are formed around large particulate organic matter (POM), followed by the inclusion of micro-aggregates within the macro-aggregates. Microbial decomposers of plant residues provide the extracellular polymeric "glue" by which mineral particles and small aggregates bind to form macro-aggregates around the POM (Phase I). Clay-sized mineral particles with relatively larger specific surface area provide complexation capacity to chemically bind constituent molecular components of SOM to the mineral surfaces, which protects the organic matter and favours inclusion of the clay-size fraction in micro- and macro-aggregate formation (Nikolaidis and Bidoglio, 2013). The macro-aggregate POM is further decomposed and the resulting finely fragmented POM is encrusted with silt-clay sized aggregates leading to the formation of micro-aggregates within macro-aggregates (AC2 in AC3) (Phase II). Decreased microbial activity inside the macro-aggregates due to decreased availability of C and energy following biodegradation of POM reduces the supply of microbial polymers and aggregate disruption occurs (Phase III) with instant release of stable AC2 and AC1 aggregates and the

186 fragmented POM becomes unprotected (Phase IV). When fresh plant residues enter the soil, new
187 macro-aggregates form and the cycle of aggregation and dis-aggregation continues.

188 [Insert Figure 2 here]

189 Figure 3 presents a schematic representation of the aggregation process of the CAST model, its
190 aggregate fractions and the C pools sequestered in them. Each arrow represents a mass transformation
191 rate that is translated mathematically by the law of mass action into a linear rate equation with a first-
192 order rate constant that defines the rate as proportional to the mass of the reactive material that is
193 being transformed. The figure shows the phases of WSA formation together with the C pools and
194 fluxes. Fresh plant residue is characterized by the decomposable (DPM) and resistant plant material
195 (RPM). Both DPM and RPM are fragmented and comprise the coarse fraction of DPMc and RPMc
196 which further break down to fine fractions DPMf and RPMf. In the initial phase of aggregation, the
197 AC3 aggregates are comprised of POM, AC1 aggregates, sand, bacteria and fungi. At the second
198 stage, coarse plant material, DPMc and RPMc is decomposed within the AC3 into fine, fragmented
199 DPMf and RPMf which further facilitates the formation of the AC2 micro-aggregates within the AC3.
200 Further biodegradation of the OM decreases the microbial activity and the stability of the macro-
201 aggregates which eventually break down into aggregates of the AC1 and AC2 size fractions.

202 [Insert Figure 3 here]

203 The CAST model has been further modified to incorporate the effect of tilling and the impact of
204 frozen soil on the aggregation/disaggregation mechanisms in order to improve the model versatility
205 and extend the conditions that can be represented by simulation of the dynamics of SOM. Tilling was
206 incorporated in the model by making the WSA destruction parameters time-variable. When there is
207 tilling, the destruction rate parameter can be changed to a higher value, depending on the tilling
208 intensity, which upon cessation of tilling subsequently reverts to its initial value. Similarly, frozen soil
209 was incorporated into the model by allowing the rate constants of aggregation and decomposition of
210 OM to vary with temperature. When the ground was defined as frozen, the rate constants of

aggregation and OM decomposition can be changed to lower values which, over time, can then revert to their normal values.

The most important input parameters of the CAST model include climatic data such as temperature, precipitation and evapotranspiration (ET), soil properties (silt and clay content and bulk density) and WSA distribution and SOC stock distribution within each of the defined fractions of WSA. More specifically, samples from the topsoil (0-10 cm) for each field site were analyzed for the AC1, AC2 and AC3 fractions of WSA according to the methodology developed by Elliott (1986). AC3 aggregates were further separated to coarse POM (POMc), sand, easily dispersed silt-clay fraction and AC2 aggregates according to Lichter et al. (2008). The AC2 aggregates within the AC3 aggregates were further separated into fine POM (POMf), sand and the silt-clay fractions. The free AC2 aggregates were also separated into POMf and silt-clay fractions. These measurements are performed for every soil sample in order to obtain parameter values both for the initialization and calibration of the model.

2.2 Site Description

The data and experimental results used in the simulations represent conditions of natural ecosystems and agricultural practices. Table 2 presents a summary of the sites and their respective management. A description of the site details follows:

Damma Glacier CZO – Switzerland

Damma Glacier CZO is located at the central Alps, Canton Uri, Switzerland and is a 9.9 km^2 catchment with an elevation range between 1940 and 3630 m above sea level. The glacier has been retreating since 1850, forming a soil chronosequence on a relatively flat area of about 1 km length at an altitude between 1950 and 2050 m. The glacier recession was reversed two times, during 1920 to 1928 and 1970 to 1992, which resulted in two small terminal moraines. Therefore, the chronosequence consists of three groups of soil ages. The youngest sites include soils from 6 to 14 years old, the intermediate group comprises of soils developed between 1930 and 1950 and the oldest group includes soils that started to evolve during 1870 to 1897. The soils have been classified as

Lithic leptosols. The soils at locations in the chronosequence, between those representing these stages of soil formation, have been eroded during glacial advances (Banwart et al., 2011; Bernasconi et al., 2011). The CAST model was used to simulate the accumulation of SOC and the development of soil structure along the chronosequence (Andrianaki et al., 2016). As the chronosequence is not continuous there were 5 simulations, 3 of the different soil ages (young soils, intermediate soils and old soils) and 2 of the readmissions of the glacier. The calibration of the models is based on the extensive dataset available for the Damma Glacier CZO and a climate reconstruction back to 1867 (Smittenberg et al., 2012).

Heilongjiang Mollisols – China

The Heilongjiang Mollisols experimental field site is located in the central region of the Mollisols in Northeast China. The experimental site was established in 2004 at the State Key Experimental Station of Agroecology, Chinese Academy of Sciences, Hailun, Heilongjiang province. The region has a typical temperate continental monsoon climate with a hot summer and cold winter. The soils have evolved from sedimentary materials of loamy loess. Parent material was removed from the C horizon (> 2 m) and replaced the surface soil down to 0.8 m. The experiment was set up to study soil development and restoration from an extremely degraded soil (Li et al., 2016). The field experiment included six treatments, two natural ecosystems and four agricultural fields, in order to compare: a) no-tilled soils under fallow and soil planted with alfalfa and b) tilled soils with rotation of soya and maize in alternate years and different combinations of mineral fertilization (F) and organic (C) amendments. More specifically the tilled soils were managed i) without fertilization and organic amendment (F0C0) after the above-ground biomass was removed, ii) with fertilization and no organic C amendment (F1C0), iii) with fertilization and low amount of organic C input (F1C1) after only partial above-ground biomass of two crops was incorporated into soil, and iv) with fertilization and high amount of organic C input (F1C2) after all the above-ground biomass of the seasonal crop was incorporated into the soil (Li et al., 2016).

Koiliaris CZO – Greece

Koiliaris River catchment is a CZO that represents severely degraded soils due to intense agricultural practices applied for many centuries. It represents typical Mediterranean dry-lands soils evolving under imminent threat of desertification. The Koiliaris CZO is located 25 km east of the city of Chania, Crete, Greece. The total watershed area is approximately 130 km^2 and the main supply of water originates from the White Mountains. An additional area of 50 km^2 outside of the Koiliaris CZO is hydro-geologically connected due to limestone bedrock-karst terrain. Water erosion is recognized as the most important soil degrading threat due to the clearing of forests and natural vegetation, the livestock overgrazing and the tilling of crops (Stamati et al., 2013a, 2013b). Simulations performed for the Koiliaris CZO included both natural ecosystem and agricultural management scenarios and the soil type is calcaric regosol.

Clear Creek – Iowa, USA

The Clear Creek site is located on the outskirts of Iowa City, USA. It is representative of humid continental climates with coarse textured (sandy loam) Mollisols. The cropping period lasts from May to September, while during the winter period the soils are covered by snow. The site has been selected to study the impacts of land use conversion, from agricultural use to natural vegetation, on soil functions (Stamati et al., 2013a, 2013b).

Slavkov Forest CZO – Czech Republic

Slavkov Forest CZO is a Protected Landscape Area located in the northwestern Czech Republic, 120 km west of Prague. The catchment area is 0.273 km^2, with elevations in the range of 829 to 949 m above sea level. There is intense silvilculture with rapidly aggrading Norway spruce monoculture stands since 1850 on nutrient-depleted soils, mostly Podzols developed on granite. The mean stand age is about 40 years, and closed canopy forest covers 82% of the CZO, while clearings with young seedlings cover 18% of the catchment. The most important threats to the soil include nutrient leaching, acidity, metal toxicity, harvest erosion and compaction, low biodiversity due to monoculture, C loss due to elevated organic C export and atmospheric deposition of anthropogenic pollutants (Banwart et al., 2011).

289 *Marchfeld CZO – Austria*

290 The study area is located in the Danube River flood plain downstream of Vienna in the "Marchfeld",
291 with little variation in topography and climate. During alpine glaciations, the Danube continuously
292 incised into the uplifting Tertiary basin fill and accumulated melt water terraces. The floodplain is
293 morphologically subdivided into two units: the recent floodplain sensu stricto and a slightly elevated
294 area covered by older fluvial deposits. The soils in the Marchfeld CZO are Chernozems and create a
295 chronosequence of soil development covering thousands of years, which allows the study of temporal
296 soil development and also the effects of various land uses. The data from Marchfeld CZO were used
297 to perform three simulations of the land use conversion (Rampazzo Todorovic et al., 2014). The initial
298 conditions for each case are freshly deposited sediments with specified soil texture but without
299 structure. Every simulation represents the evolution of C sequestration and soil structure development.
300 The first 200 years of each simulation represent the forest development. The term "*Forest"* refers to
301 the simulation of subsequent steady-state climax forest for 400 years. The term *"Cropland"* refers to
302 the simulation of land use conversion from forest (initial 200 years) to cropland (total 400 years), and
303 the term "*Grassland"* refers to the simulation of land use conversion from forest (initial 200 years) to
304 grassland (total 400 years). The lengths of these periods were inferred from land use history.

305 *Milia – Greece*

306 Milia represents a strongly eroded Eutric Lithosol soil in which restoration practices including
307 terraces formation and incorporation of organic amendments have been applied. The elevation of the
308 study area is 500 m above sea level. Soil samples were collected from three terraces subjected to
309 cultivation with varying compost application practices. Simulations were performed to represent a 10
310 year period of farming operations (Vavlas et al., 2014). The frequency of compost application was
311 twice per year, through tilling, corresponding to a total application of 8 t C/ha. For terrace 1 (Milia 1),
312 the compost was applied annually for 10 years, while for terrace 2 (Milia 2) it was applied for 8 years
313 followed by 2-years fallow. Finally, for terrace 3 (Milia 3), the organic amendment was applied once
314 every 3 years.

315 [Insert Table 2 here]

316 ## 3. Results and Discussion

317 The interpretation of soil properties, climatic conditions, and land use and management practices in
318 the study areas reveals great variability. The sites are characterized by variable climatic conditions
319 ranging from 0-4 ^{o}C of mean annual temperature of Damma Glacier CZO to 17.6-18.1 ^{o}C of the
320 Greek sites. Precipitation also varies from 1898 mm/yr of Damma Glacier CZO to 510 mm/yr of the
321 Heilongjiang Mollisols. In addition, the sites cover a wide variety of soil types at different stages of
322 soil development, from lithic leptosol of Damma Glacier to eutric lithosols of Milia, to calcaric
323 regosols of Koiliaris and then to more developed podsols, chernozems and mollisols of Slavkov
324 forest, Marchfeld and China/USA respectively. Organic carbon input to the soils at the natural
325 ecosystem sites was approximately proportional to the temperature gradient as it is shown in the site
326 data comparison of Table 3. The lowest C inputs occurred at the Damma Glacier CZO and the
327 Heilongjiang Mollisols and approached 1 t C/ha/yr as a consequence of the short growing season
328 imposed by the low temperatures. As the annual average temperature increases to 5.3 ^{o}C in Slavkov
329 Forest CZO, the C input also increased to 2.75 t C/ha/yr. For higher temperatures, such as that of
330 Clear Creek with 10.3 ^{o}C and of Koiliaris CZO 18.1 ^{o}C, the amount of C inputs was strongly mediated
331 by the precipitation level and its seasonal distribution. For instance, the C input of Clear Creek was
332 5.8 t C/ha/yr due to the availability of precipitation during the summer (923 mm/yr) whereas in
333 Koiliaris CZO is 3.8 t C/ha/yr due to semi-arid climate (652 mm/yr). Organic carbon input to soils at
334 the agricultural sites depends on the applied management practices; e.g. tilling intensity, below
335 ground biomass of from crop production, and the amount of above ground biomass incorporated to
336 the soil. At these sites, annual C input varies from 0.205 tC/ha at Marchfeld to 8 tC/ha at Milia.

337 [Insert Table 3 here horizontally]

338 A schematic diagram of the study sites placed along a temperature gradient representing different
339 stages of soil evolution is illustrated in Figure 4. The sites are placed according to the annual mean
340 temperature, beginning from the Heilongjiang Mollisols and Damma Glacier CZO, to Slavkov Forest
341 CZO, Marchfeld CZO, Clear Creek ending to Milia and Koiliaris CZO. The initial soil conditions for
342 the model simulations of each site, in terms of clay and macro-aggregate content, and the rates of

343 macro-aggregates formation and decomposition of plant litter are also illustrated in Figure 4. The
344 insert in each site are the C flux balances which include C input, C storage and CO_2 emissions. The
345 ordering of sites according to temperature also coincides with the different stages of soil evolution
346 starting from soil formation due to weathering in Damma Glacier CZO and the parent material of
347 Heilongjiang Mollisols, moving to soils used for forestry at Slavkov Forest CZO and arable land at
348 Marchfeld CZO, ending at the relatively degraded soils of Clear Creek and Koiliaris CZO due to
349 permanent cropping and overgrazing. The C flux balances show soil degradation due to C losses
350 represented by the negative values of C storage. The site of Milia is placed outside the circle of soil
351 formation and soil degradation because it represents soil restoration conditions due to organic carbon
352 addition.

353 [Insert Figure 4 here]

354 3.1 Calibration results

355 The simulations for the Koiliaris CZO, Clear Creek, Marchfeld CZO, and Slavkov Forest CZO sites
356 with regard to the distribution of SOC stocks and WAS, and their interpretation with the field data
357 used for model calibration, are shown in Figure 5a and Figure 5b respectively. The calibration
358 parameters of the CAST model and their description are summarized in Table 4.The descriptions of
359 the parameters indicating soil initial conditions are presented in Table SI 1 (Appendix –
360 Supplementary Information).
361 [Insert Table 4 here]
362 [Insert Figure 5a here]
363 [Insert Figure 5b here]

364 A comparison of the CO_2 fluxes, C stocks, and microbial biomass is presented in Table 5. The table
365 presents the initial C content of each site that ranges from 0.6-14.8 t C/ha at Damma Glacier CZO to
366 13.5 t C/ha for the Heilongjiang Mollisols to 55.4 t C/ha for Slavkov Forest, to 18.5 t C/ha for Clear
367 Creek and 34.9 t C/ha for Koiliaris CZO soil, for the natural sites. Regarding the agricultural sites, the
368 initial SOC mass ranges from 13.77 t C/ha for the Heilongjiang Mollisols to 58.55 t C/ha for Koiliaris

CZO soil. Milia had an initial SOC mass of 33.9 t C/ha, Clear Creek 32.38 t C/ha and Marchfeld CZO 27.11 t C/ha. The values of initial SOC mass of Damma Glacier CZO and Heilongjiang Mollisols can be explained by the fact that Damma Glacier CZO is a very new, 150-year-old, soil, while the Heilongjiang Mollisols were C horizon soil brought to the soil surface and placed under cultivation. The high value for Slavkov Forest CZO is due to the fact that it is a forested site relatively undisturbed for the past 70 years, while the low value of Clear Creek is due to intense cultivation of the Iowa, USA soils and the sandy / low clay content nature of the soil that offers limited mineral surface for binding and forming organo-mineral complexes that protect and sequester OM. Finally, the initial SOC mass of Koiliaris CZO is indicative of its relatively high clay content and lower intensity of agricultural practices.

[Insert Table 5 here horizontally]

Regarding the natural ecosystems, the young soils of Damma Glacier CZO and Heilongjiang Mollisols sequester higher amounts of the C input, up to 0.31 (28%) and 0.47 t C/h/yr (40%) respectively, while the older soils of the Clear Creek and Koiliaris CZO sequester significant lower proportions, 5% and 13% respectively even though the annual storage is maintained close to that of the young soils (0.27 t C/ha/yr for Clear Creek and 0.48 t C/ha/yr for Koiliaris CZO). These differences can be explained by climatic conditions, soil structure and land use management. Slavkov Forest CZO presents intermediate values with 26% (0.72 t C/ha/yr) of the C input to sequestered annually. The CO_2 emissions follow the opposite trend to that observed for C storage with the young soils having lower emissions compared to the older soils. As for the cultivated sites, the initial SOC mass (Table 3) ranged from 13.77 t C/ha for the Heilongjiang Mollisols to 58.55 t C/ha for Koiliaris CZO soil. Milia had an initial SOC mass of 33.9 t C/ha, Clear Creek 32.38 t C/ha and Marchfeld CZO 27.11 t C/ha. The values of initial SOC mass of Heilongjiang Mollisols can be explained by the fact that the Heilongjiang Mollisols had a well-developed C horizon when the cultivation started. C input ranged from 0.2 t C/ha at Marchfeld to 8 t C/ha in Milia. The data from the Heilongjiang Mollisols showed that the higher the C input, the more the C storage, CO_2 emissions and bacterial biomass. A similar trend was found for the Milia soils. Comparison of sites with similar C input such as the

396 Koiliaris CZO and Marchfeld CZO revealed that climate (i.e. temperature, rainfall) and water
397 availability through irrigation played an important role. The warmer site (Koiliaris CZO) showed
398 higher CO_2 emissions and loss of organic C despite the lower bacterial stock. Similar emissions of
399 CO_2 to those observed in the Koiliaris CZO were observed in the Heilongjiang Mollisols which could
400 be attributed to the higher C input.

401 The poor soil structure of the Heilongjiang Mollisols and the Damma Glacier CZO seems to improve
402 with time. This is evident in the Damma Glacier CZO chronosequence where the macro-aggregate
403 AC3 fraction increases from 15% to 46%. In the Heilongjiang Mollisols the macro-aggregate fraction
404 ranged between 29-35%. Even greater proportions of macro-aggregates were found in the Clear Creek
405 and Slavkov Forest CZO soils that approached 79% and 78% respectively. The corresponding
406 proportion for the Koiliaris CZO scrublands was 47%. Finally, in the forests and grasslands of the
407 Marchfeld CZO the macro-aggregate fraction was 45% and 57% respectively.

408 Regarding the cultivated sites, the Heilongjiang Mollisols macro-aggregate fraction ranged from 21%
409 to 48% depending on the management practice. Milia macro-aggregate fractions ranged from 45% to
410 70% with the highest proportions corresponding to the treatment of the annual application of organic
411 matter amendment. Finally, the Koiliaris CZO macro-aggregate fraction was 53%, Clear Creek was
412 74% and Marchfeld CZO was 23%, again reflecting differences regarding climate, agricultural
413 practices and soil properties. A decrease in the macro-aggregate fractionation was observed in
414 Koiliaris CZO natural ecosystem, which was accompanied by an increase in the micro-aggregate
415 fraction AC2. The site of Marchfeld CZO showed a large (277%) increase in AC3 content the first
416 200 years of forest development, since the site initially was consisted of sediment depositions, with no
417 aggregates and soil structure.

418 The values for the calibration parameters of the CAST model for the simulations of natural
419 ecosystems and agricultural sites are summarized in Table SI 2 and Table SI 3 respectively, while a
420 range of these values is presented in Table SI 4 in order to provide an initial database for future
421 modeling activities. Overall, the modeling results of the CAST model for both the natural ecosystems

and agricultural management sites were consistent with the field data. The model has been able to describe SOC and soil structure dynamics in a wide variety of natural ecosystem and agricultural sites around the world. A broad comparison between the process rates constants of the agricultural management sites and the natural ecosystems shows that the rates of fragmentation, micro aggregation and disruption are higher for the agricultural sites, while the rates for macro aggregation and decomposition of organic matter are higher for the natural ecosystems.

3.2 Factors controlling soil structure dynamics and carbon sequestration

Our findings confirmed those of earlier studies that the factors regulating the sequestration of C in soils are driven by complex interactions within the soil-plant-water system. A principal component statistical analysis (PCA) was employed to classify the soils studied in the present work in terms of their status considering climatic parameters, basic soil properties, SOC and macro-aggregate content at the initial and final stages of simulation and their annual rates of change, C input rates to soil through litter fall and organic amendments, the decomposition rates of the soil C pools, and the magnitude of disruption of the aggregates including the impact of tilling.

The score and the loading plots of the components of the PCA are presented in Figures 6 and 7 in order to illustrate the clustering of the sites and the significance of each parameter in this clustering. The 35 parameters used in the PCA together with the eigenvalues for the first two principal components are summarized in Table SI 5. The most important parameters that explained the variability in the first component are: the initial macro-aggregate fraction as percentage of total mass, the initial value of the SOC normalized to the mass content of the silt and clay, the temperature, the bulk density and the ET. Similarly, the most important parameters included in the second component are: the percent mass fraction of macro-aggregates, the percent mass fraction of silt-sized aggregates, the decomposition rates of humified and bacterial organic C pools, and the fragmentation rate of resistant plant material by soil fauna. PC1 could explain 32.1% of the variability of the samples, while together with PC2 49.7% of the variability.

447 Figure 6 presents the clustering of the sites as a result of the PCA. A plot of PC1 versus PC2 of all the
448 sites resulted in the development of four clusters. The first cluster includes the sites of Heilongjiang
449 Mollisols (all management practices) and Damma Glacier CZO (new and intermediate soils) which
450 represents soils at their early stage of evolution. For the Heilongjiang Mollisols, this reflects the
451 introduction of C horizon parent material to the soil surface, hence exhibiting characteristics of a
452 young soil. The second cluster includes all the sites of Marchfeld CZO, Slavkov Forest CZO, Damma
453 Glacier CZO (older soils) and the natural ecosystems of Koiliaris CZO. These sites are either natural
454 or set aside sites or flood plain soils with a high degree of fertility. The third cluster includes the
455 agricultural sites of the Koiliaris CZO and all the Clear Creek studies which represent intensively
456 managed soils. Finally, the fourth cluster includes the site of Milia (all management practices) where
457 intensive C sequestration occurs due to large C additions. As it can be seen from Figure 6, PC1
458 differentiates the sites starting from the left with soils at an early stage of evolution, moving to the
459 second cluster in the middle with mature soils and moving to the upper right of the graph with the
460 intensively managed soils. PC2 differentiates the sites based on the degree of intensification versus
461 natural ecosystem sites but with C addition. Cluster 4 accounts for the Milia site which diverges from
462 the main trend of clusters 1 through 3 due to extensive C addition. Similarly, the sites within cluster
463 1 identify a trend from the early diagenesis sites of Damma Glacier CZO to the cultivated C horizon
464 sites of the Heilongjiang Mollisols. It is interesting to note that PC2 differentiates the Chinese
465 Heilongjiang Mollisols based on the amount of C added.

466 [Insert Figure 6 here]

467 In terms of soil carbon evolution, the four clusters of Figure 6 represent the sites dominated by carbon
468 fixation (Cluster 1), the sites with stable SOC content (Cluster 2), the sites dominated by SOC
469 mineralization and net loss (Cluster 3) and the sites with large artificial SOC addition (Cluster 4).

470 Figure 7 presents the Loading Plot of the PCA analysis in order to identify the most important
471 parameters contributing to the differentiation of the clusters. The factors contributing to the
472 differentiation of Cluster 1 includes bacterial biomass as a proxy for microbial decomposer activity,

SOC storage, the increase of the fertility factor SOC/(silt + clay) and the increase of the macro-aggregate fraction. Cluster 2 represents older soils which have probably reached a steady state. This cluster is placed in the middle of the diagram where all the factors play a seemingly equal role. Cluster 3 represents degraded soils where the decomposition rates of the C pools is higher, the decomposable plant material outweighs the resistant plant material and the disruption of macro-aggregates is increased. Cluster 4 represents soils restored by beneficial intervention practices where the aggregation rates are higher, the plant material is decomposed by fauna and contributes to aggregation. The trend presented in the PCA analysis in Figure 6 is related to the evolutionary nature of the soils beginning from the young soils and parent material, proceeding to the older soils, forests and arable lands, ending either at soil degradation through continuous cultivation or to restoration through beneficial practices of previously intensively managed soils. In broad terms the evolution of soil structure and increasing intensity of human exploitation of the resulting soil functions correlates with the trajectory shown in Figure 6. This trajectory starts from young soils at the left, to productive soils in the centre, to heavily impacted and very intensively managed soils at the upper right. The dotted arrows show the trend of soil evolution within each CZO. For the Heilongjiang Mollisols, the trend starts at the natural ecosystems ending at the cultivation practices. For the Damma Glacier CZO soils, it begins at the young soils, ending at the older soils. For the Marchfeld CZO soils the trend starts at the grassland, moving to forest, ending at the agricultural land. At Koiliaris CZO and Clear Creek the trend starts at natural ecosystem ending at cultivation. At Milia the trend of soil restoration starts at low C amendment addition ending at higher application. It appears that the first two principal components can account for the variability that describes the evolutionary nature of soil from formation to cultivation as well as a reverse in this trajectory when moving from intensive utilization with soil degradation to restoration.

[Insert Figure 7 here]

Figure 7 presents the variables with the higher values, either positive or negative, of the factors with the higher impact on soil structure dynamics and C sequestration. These variables include soil bulk density, clay content, temperature, ET, initial SOC mass and AC3 fraction, decomposition rates of the

BIO and HUM pools, the contribution of plant litter and silt clay sized aggregates on AC2 and AC3 formation, the formation rate of AC3 aggregates and the fragmentation of resistant plant material through fauna. Briefly the factors controlling soil structure and C dynamics are related to soil properties, climatic conditions, decomposition rates of organic matter, and formation rates and the predominant buildersers of macro aggregates.

4. Conclusions

In this study, the CAST model was modified to incorporate the impact of tilling and frozen soil conditions on aggregate formation and SOC sequestration. The modified CAST model was used to simulate 20 cases of different soil management practices located at 7 sites across a wide range of climatic conditions, land uses, and parent material. The CAST model can successfully simulate and predict aggregate formation and C sequestration on soils across the world, under a variety of climatic, lithological and agricultural conditions. The principal component analysis indicated the predominant factors controlling soils structure and C sequestration to be the plant litter contribution to aggregate formation, the decomposition rates of the humified and bacterial C pools, the initial state of soil in terms of SOC, silt and clay and macro-aggregate contents, the fragmentation rate of plant material through earthworms and other fauna, the macro-aggregate formation rates, the temperature and evapotranspiration and the soil bulk density. The model reliably simulated soil C and soil structure dynamics for a wide variety of land uses, climatic and lithological conditions and soil properties providing support for the underlying conceptual and mathematical model and evidence that the CAST model provides a valuable quantitative analysis tool to interpret soil structure formation processes and to aid the design of sustainable soil management practices which support WSA formation.

Acknowledgment

Funding for this work was provided by the EU FP7-ENV-2009 Project SoilTrEC ‘‘Soil Transformations in European Catchments’’ (Grant #244118).

References

Abiven, S., Menasseri, S., Angers, D.A., Leterme, P., 2008. A Model to Predict Soil Aggregate Stability Dynamics following Organic Residue Incorporation under Field Conditions. Soil Sci. Soc. Am. J. 72, 119–125. doi:10.2136/sssaj2006.0018

Abiven, S., Menasseri, S., Chenu, C., 2009. The effects of organic inputs over time on soil aggregate stability - A literature analysis. Soil Biol. Biochem. doi:10.1016/j.soilbio.2008.09.015

Álvaro-Fuentes, J., Paustian, K., 2010. Potential soil carbon sequestration in a semiarid Mediterranean agroecosystem under climate change: Quantifying management and climate effects. Plant Soil 338, 261–272. doi:10.1007/s11104-010-0304-7

Andrianaki, M., Bernasconi, S.M., Nikolaidis, N.P., 2016. Application of the Roth-C and CAST models for the modelling of soil organic carbon and soil structure dynamics at the Damma Glacier CZO, in: Advances in Agronomy.

Banwart, S., Bernasconi, S.M., Bloem, J., Blum, W., Brandao, M., Brantley, S., Chabaux, F., Duffy, C., Kram, P., Lair, G., Lundin, L., Nikolaidis, N., Novak, M., Panagos, P., Ragnarsdottir, K. V, Reynolds, B., Rousseva, S., de Ruiter, P., van Gaans, P., van Riemsdijk, W., White, T., Zhang, B., 2011. Soil processes and func tions in critical zone observatories: Hypotheses and experimental design. Vadose Zo. J. 10, 974–987. doi:10.2136/vzj2010.0136\r10.1002/hyp.7380; Beddington, J., (2009) Food, Energy, Water and the Climate: A Perfect Storm of Global Events?, , Government Office for Science, London; Bernasconi, S.M., Weathering, soil formation and initial ecosystem evolution on a glacier forefield: A case study from the Damma Glacier (2008) Switzerland. Mineral. Mag., 72, pp. 19-22. , BigLink Project Members, doi:10.1180/minmag.2008.072.1.19; Bernasconi, S.M., Bauder, A., Bourdon, B., Brunner, I., Bünemann, E., Christ

Banwart, S., Bernasconi, S.M., Bloem, J., Blum, W., Brandao, M., Brantley, S., Chabaux, F., Duffy, C., Kram, P., Lair, G., Lundin, L., Nikolaidis, N., Novak, M., Panagos, P., Ragnarsdottir, K.V.,

550 Reynolds, B., Rousseva, S., de Ruiter, P., van Gaans, P., van Riemsdijk, W., White, T., Zhang,
551 B., 2011. Soil Processes and Functions in Critical Zone Observatories: Hypotheses and
552 Experimental Design. Vadose Zo. J. 10, 974–987. doi:10.2136/vzj2010.0136

553 Bernasconi, S.M., Bauder, A., Bourdon, B., Brunner, I., Bünemann, E., Chris, I., Derungs, N.,
554 Edwards, P., Farinotti, D., Frey, B., Frossard, E., Furrer, G., Gierga, M., Göransson, H., Gülland,
555 K., Hagedorn, F., Hajdas, I., Hindshaw, R., Ivy-Ochs, S., Jansa, J., Jonas, T., Kiczka, M.,
556 Kretzschmar, R., Lemarchand, E., Luster, J., Magnusson, J., Mitchell, E. a. D., Venterink, H.O.,
557 Plötze, M., Reynolds, B., Smittenberg, R.H., Stähli, M., Tamburini, F., Tipper, E.T., Wacker, L.,
558 Welc, M., Wiederhold, J.G., Zeyer, J., Zimmermann, S., Zumsteg, A., 2011. Chemical and
559 Biological Gradients along the Damma Glacier Soil Chronosequence, Switzerland. Vadose Zo.
560 J. 10, 867–883. doi:10.2136/vzj2010.0129

561 Brantley, S.L., Goldhaber, M.B., Vala Ragnarsdottir, K., 2007. Crossing disciplines and scales to
562 understand the critical zone. Elements 3, 307–314. doi:10.2113/gselements.3.5.307

563 Carvalho Leite, L.F., De Sá Mendonça, E., Oliveirade De Almeida MacHado, P.L., Inácio Fernandes
564 Filho, E., Lima Neves, J.C., 2004. Simulating trends in soil organic carbon of an Acrisol under
565 no-tillage and disc-plow systems using the Century model. Geoderma 120, 283–295.
566 doi:10.1016/j.geoderma.2003.09.010

567 CEC, 2006. Thematic strategy for soil protection. Com 12.

568 Coleman, K., Jenkinson, D.S., 1999. RothC-26.3 - A Model for the turnover of carbon in soil: Model
569 description and windows users guide: November 1999 issue. Lawes Agricultural Trust
570 Harpenden. ISBN 0 951 4456 8 5.

571 Dou, F., Wight, J.P., Wilson, L.T., Storlien, J.O., Hons, F.M., Sainju, U.M., 2014. Simulation of
572 biomass yield and soil organic carbon under bioenergy sorghum production. PLoS One 9.
573 doi:10.1371/journal.pone.0115598

574 Elliott, E.T., 1986. Aggregate structure and carbon, nitrogen, and phosphorus in native and cultivated

575 soils. Soil Sci. Soc. Am. J. 627–633.

576 Finke, P.A., 2012. Modeling the genesis of luvisols as a function of topographic position in loess
577 parent material. Quat. Int. 265, 3–17. doi:10.1016/j.quaint.2011.10.016

578 Finke, P.A., Hutson, J.L., 2008. Modelling soil genesis in calcareous loess. Geoderma 145, 462–479.
579 doi:10.1016/j.geoderma.2008.01.017

580 Galdos, M. V., Cerri, C.C., Cerri, C.E.P., Paustian, K., Van Antwerpen, R., 2009. Simulation of Soil
581 Carbon Dynamics under Sugarcane with the CENTURY Model. Soil Sci. Soc. Am. J. 73, 802–
582 811. doi:10.2136/sssaj2007.0285

583 GAO, C. sheng, WANG, J. guo, ZHANG, X. yi, SUI, Y. yu, 2008. The Evolution of Organic Carbon
584 in Chinese Mollisol Under Different Farming Systems: Validation and Prediction by Using
585 Century Model. Agric. Sci. China 7, 1490–1496. doi:10.1016/S1671-2927(08)60407-1

586 General Assembly, United Nations, 2015. Transforming our world: The 2030 agenda for sustainable
587 development,
588 https://sustainabledevelopment.un.org/content/documents/7891Transforming%20Our%20World
589 . pdf. doi:10.1007/s13398-014-0173-7.2

590 Gilhespy, S.L., Anthony, S., Cardenas, L., Chadwick, D., del Prado, A., Li, C., Misselbrook, T., Rees,
591 R.M., Salas, W., Sanz-Cobena, A., Smith, P., Tilston, E.L., Topp, C.F.E., Vetter, S., Yeluripati,
592 J.B., 2014. First 20 years of DNDC (DeNitrification DeComposition): Model evolution. Ecol.
593 Modell. 292, 51–62. doi:10.1016/j.ecolmodel.2014.09.004

594 Goglio, P., Grant, B.B., Smith, W.N., Desjardins, R.L., Worth, D.E., Zentner, R., Malhi, S.S., 2014.
595 Impact of management strategies on the global warming potential at the cropping system level.
596 Sci. Total Environ. 490, 921–933. doi:10.1016/j.scitotenv.2014.05.070

597 Jastrow, J.D., Amonette, J.E., Bailey, V.L., 2007. Mechanisms controlling soil carbon turnover and
598 their potential application for enhancing carbon sequestration. Clim. Change 80, 5–23.

599 doi:10.1007/s10584-006-9178-3

600 Jenkinson, D.S., 1990. The Turnover of Organic Carbon and Nitrogen in Soil. Philos. Trans. R. Soc.
601 London Ser. B-Biological Scienses 329, 361–368. doi:10.1098/rstb.1990.0177

602 Jenkinson, D.S., Coleman, K., 2008. The turnover of organic carbon in subsoils. Part 2. Modelling
603 carbon turnover. Eur. J. Soil Sci. 59, 400–413. doi:10.1111/j.1365-2389.2008.01026.x

604 Keating, B.A., Carberry, P.S., Hammer, G.L., Probert, M.E., Robertson, M.J., Holzworth, D., Huth,
605 N.I., Hargreaves, J.N.G., Meinke, H., Hochman, Z., McLean, G., Verburg, K., Snow, V., Dimes,
606 J.P., Silburn, M., Wang, E., Brown, S., Bristow, K.L., Asseng, S., Chapman, S., McCown, R.L.,
607 Freebairn, D.M., Smith, C.J., 2003. An overview of APSIM, a model designed for farming
608 systems simulation, in: European Journal of Agronomy. pp. 267–288. doi:10.1016/S1161-
609 0301(02)00108-9

610 Kotronakis, M., Giannakis, G. V., Nikolaidis, N.P., Rowe, E.C., Valstar, J., Paranychianakis, N. V.,
611 Banwart, S.A., 2016. Modeling the impact of carbon amendments on soil structure, nutrient
612 dynamics and plant growth using the 1D-ICZ model, in: Advances in Agronomy. p. In this book.

613 Lal, R., 2015. Restoring soil quality to mitigate soil degradation. Sustain. 7, 5875–5895.
614 doi:10.3390/su7055875

615 Lal, R., 2013. Food security in a changing climate. Ecohydrol. Hydrobiol. 13, 8–21.
616 doi:10.1016/j.ecohyd.2013.03.006

617 Lal, R., 2004. Soil carbon sequestration impacts on global climate change and food security. Science
618 304, 1623–1627. doi:10.1126/science.1097396

619 Li, C., Trettin, C., Sun, G., McNulty, S., Butterbach-Bahl, K., 2005. Modeling carbon and nitrogen
620 biogeochemistry in forest ecosystem. Int. Nitrogen Conf. 893–898.

621 Li, S., Li, Y., Li, X., Tian, X., Zhao, A., Wang, S., Wang, S., Shi, J., 2016. Effect of straw
622 management on carbon sequestration and grain production in a maize-wheat cropping system in

623 Anthrosol of the Guanzhong Plain. Soil Tillage Res. 157, 43–51. doi:10.1016/j.still.2015.11.002

624 Liao, Y., Wu, W.L., Meng, F.Q., Smith, P., Lal, R., 2015. Increase in soil organic carbon by
625 agricultural intensification in northern China. Biogeosciences 12, 1403–1413. doi:10.5194/bg-
626 12-1403-2015

627 Lichter, K., Govaerts, B., Six, J., Sayre, K.D., Deckers, J., Dendooven, L., 2008. Aggregation and C
628 and N contents of soil organic matter fractions in a permanent raised-bed planting system in the
629 Highlands of Central Mexico. Plant Soil 305, 237–252. doi:10.1007/s11104-008-9557-9

630 Luo, Z., Wang, E., Bryan, B.A., King, D., Zhao, G., Pan, X., Bende-Michl, U., 2013. Meta-modeling
631 soil organic carbon sequestration potential and its application at regional scale. Ecol. Appl. 23,
632 408–420. doi:10.1890/12-0672.1

633 Malamoud, K., McBratney, A.B., Minasny, B., Field, D.J., 2009. Modelling how carbon affects soil
634 structure. Geoderma 149, 19–26. doi:10.1016/j.geoderma.2008.10.018

635 Milne, E., Banwart, S.A., Noellemeyer, E., Abson, D.J., Ballabio, C., Bampa, F., Bationo, A., Batjes,
636 N.H., Bernoux, M., Bhattacharyya, T., Black, H., Buschiazzo, D.E., Cai, Z., Cerri, C.E., Cheng,
637 K., Compagnone, C., Conant, R., Coutinho, H.L.C., de Brogniez, D., Balieiro, F. de C., Duffy,
638 C., Feller, C., Fidalgo, E.C.C., da Silva, C.F., Funk, R., Gaudig, G., Gicheru, P.T., Goldhaber,
639 M., Gottschalk, P., Goulet, F., Goverse, T., Grathwohl, P., Joosten, H., Kamoni, P.T., Kihara, J.,
640 Krawczynski, R., La Scala, N., Lemanceau, P., Li, L., Li, Z., Lugato, E., Maron, P.A., Martius,
641 C., Melillo, J., Montanarella, L., Nikolaidis, N., Nziguheba, G., Pan, G., Pascual, U., Paustian,
642 K., Pineiro, G., Powlson, D., Quiroga, A., Richter, D., Sigwalt, A., Six, J., Smith, J., Smith, P.,
643 Stocking, M., Tanneberger, F., Termansen, M., van Noordwijk, M., van Wesemael, B., Vargas,
644 R., Victoria, R.L., Waswa, B., Werner, D., Wichmann, S., Wichtmann, W., Zhang, X., Zhao, Y.,
645 Zheng, J., Zheng, J., 2015. Soil carbon, multiple benefits. Environ. Dev. 13, 33–38.
646 doi:10.1016/j.envdev.2014.11.005

647 Na Li, Mengyang You, Sotiria K.Panakoulia, Nikolaos P. Nikolaidis, Xiao-Zeng Hana, B.Z., 2016.

Soil aggregate formation and organic carbon turnover shifted among different land uses and agricultural practices during the early pedogenesis of a Mollisol, in: Advances in Agronomy.

Nadeu, E., Gobin, A., Fiener, P., van Wesemael, B., van Oost, K., 2015. Modelling the impact of agricultural management on soil carbon stocks at the regional scale: The role of lateral fluxes. Glob. Chang. Biol. 21, 3181–3192. doi:10.1111/gcb.12889

Nelson, E., Mendoza, G., Regetz, J., Polasky, S., Tallis, H., Cameron, D.R., Chan, K.M.A., Daily, G.C., Goldstein, J., Kareiva, P.M., Lonsdorf, E., Naidoo, R., Ricketts, T.H., Shaw, M.R., 2009. Modeling multiple ecosystem services, biodiversity conservation, commodity production, and tradeoffs at landscape scales. Front. Ecol. Environ. 7, 4–11. doi:10.1890/080023

Nikolaidis, N.P., Bidoglio, G., 2013. Soil Organic Matter Dynamics and Structure. Sustain. Agric. Rev., Sustainable Agriculture Reviews 12, 175–199. doi:10.1007/978-94-007-5961-9_6

Parton, W.J., Schimel, D.S., Cole, C. V., Ojima, D.S., 1987. Analysis of factors controlling soil organic matter levels in Great Plains grasslands. Soil Sci. Soc. Am. J. 51, 1173–1179. doi:10.2136/sssaj1987.03615995005100050015x

Poeplau, C., Don, A., 2015. Carbon sequestration in agricultural soils via cultivation of cover crops - A meta-analysis. Agric. Ecosyst. Environ. 200, 33–41. doi:10.1016/j.agee.2014.10.024

Rampazzo Todorovic, G., Lair, G.J., Blum, W.E.H., 2014. Modeling and prediction of C dynamics in soil chronosequences of the critical zone observatory (CZO) Marchfeld/Austria. Catena 121, 53–67. doi:10.1016/j.catena.2014.05.002

Ross, C.W., Grunwald, S., Myers, D.B., Xiong, X., 2015. Land use, land use change and soil carbon sequestration in the St. Johns River Basin, Florida, USA. Geodrs 7, 19–28. doi:10.1016/j.geodrs.2015.12.001

Segoli, M., De Gryze, S., Dou, F., Lee, J., Post, W.M., Denef, K., Six, J., 2013. AggModel: A soil organic matter model with measurable pools for use in incubation studies. Ecol. Modell. 263, 1–

672 9. doi:10.1016/j.ecolmodel.2013.04.010

673 Six, J., Paustian, K., Elliott, E.T., Combrink, C., 2000. Soil structure and organic matter: I.
674 Distribution of aggregate-size classes and aggregate-associated carbon. Soil Sci. Soc. Am. J. 64,
675 681–689. doi:10.2136/sssaj2000.642681x

676 Smith, P., Smith, J.U., Powlson, D.S., McGill, W.B., Arah, J.R.M., Chertov, O.G., Coleman, K.,
677 Franko, U., Frolking, S., Jenkinson, D.S., Jensen, L.S., Kelly, R.H., Klein-Gunnewiek, H.,
678 Komarov, A.S., Li, C., Molina, J.A.E., Mueller, T., Parton, W.J., Thornley, J.H.M., Whitmore,
679 A.P., 1997. A comparison of the performance of nine soil organic matter models using datasets
680 from seven long-term experiments. Geoderma 81, 153–225. doi:10.1016/S0016-7061(97)00087-
681 6

682 Smittenberg, R.H., Gierga, M., Göransson, H., Christl, I., Farinotti, D., Bernasconi, S.M., 2012.
683 Climate-sensitive ecosystem carbon dynamics along the soil chronosequence of the Damma
684 glacier forefield, Switzerland. Glob. Chang. Biol. 18, 1941–1955. doi:10.1111/j.1365-
685 2486.2012.02654.x

686 Stamati, F.E., Nikolaidis, ikolaos P., Banwart, S., Blum, W.E.H., 2013a. A coupled carbon,
687 aggregation, and structure turnover (CAST) model for topsoils. Geoderma 211-212, 51–64.
688 doi:10.1016/j.geoderma.2013.06.014

689 Stamati, F.E., Nikolaidis, N.P., Schnoor, J.L., 2013b. Modeling topsoil carbon sequestration in two
690 contrasting crop production to set-aside conversions with RothC – Calibration issues and
691 uncertainty analysis. Agric. Ecosyst. Environ. 165, 190–200. doi:10.1016/j.agee.2012.11.010

692 Tiessen, H., Cuevas, E., Chacon, P., 1994. The Role of Soil Organic-Matter in Sustaining Soil
693 Fertility. Nature 371, 783–785. doi:10.1038/371783a0

694 Tisdall, J., Oades, J., 1982. Organic matter and water stable aggregates in soils. J. soil Sci. 33, 141–
695 163.

696 Udom, B.E., Nuga, B.O., Adesodun, J.K., 2016. Water-stable aggregates and aggregate-associated
697 organic carbon and nitrogen after three annual applications of poultry manure and spent
698 mushroom wastes. Appl. Soil Ecol. 101, 5–10.
699 doi:http://dx.doi.org/10.1016/j.apsoil.2016.01.007

700 Vavlas N.C., Nikolaidis N.P., Paranychianakis N., K.M., 2014. Modeling of soil structure and soil
701 carbon sequestration in intensively cultivated fields using organic amendments. Proc. 12th Int.
702 Conf. Prot. Restor. Environ. 377–384.

703 Zhang, L., Zhuang, Q., Li, X., Zhao, Q., Yu, D., Liu, Y., Shi, X., Xing, S., Wang, G., 2016. Carbon
704 sequestration in the uplands of Eastern China: An analysis with high-resolution model
705 simulations. Soil Tillage Res. 158, 165–176. doi:http://dx.doi.org/10.1016/j.still.2016.01.001

706

Tables

Table 1: Natural ecosystems (non tilled soils) and agricultural fields (tilled soils) of the study sites

Natural Ecosystems	Agricultural Fields
Koiliaris CZO – Calcaric Regosols - Set aside field	Koiliaris CZO – Calcaric Regosols - Cropland
Marchfeld CZO – Chernozems - Forest development	Marchfeld CZO – Chernozems -Land use conversion from forest to cropland
Marchfeld CZO – Chernozems - Land use conversion from forest to grassland	
Slavkov Forest CZO – Podsols - Forestry	
Damma Glacier CZO - Lithic Leptosols	
Heilongjiang Mollisols: 2 fields with Natural Fallow and Alfalfa	Heilongjiang Mollisols: 4 fields with Soybean –Maize rotation
Clear Creek – Millisols - Set aside field	Clear Creek – Mollisols - Cropland
	Milia: Eutric Lithosols - 3 fields with different practices of compost application - Tilling

Table 2: Summary of sites simulated with a description of soil management

Site - Treatment	Description
Heilongjiang Mollisols - NatF	Natural fallow – No fertilization, Organic Input, No Tilling
Heilongjiang Mollisols - Alfa	Alfalfa – No fertilization, Organic Input, No Tilling
Heilongjiang Mollisols - F0C0	Soybean-maize rotation –– No fertilization, No Organic Input, Tilling
Heilongjiang Mollisols - F1C0	Soybean-maize rotation –– Fertilization, No Organic Input, Tilling
Heilongjiang Mollisols - F1C1	Soybean-maize rotation –– Fertilization, Low Organic Input, Tilling
Heilongjiang Mollisols - F1C2	Soybean-maize rotation –– Fertilization, High Organic Input, Tilling
Koiliaris Natural	Koiliaris set aside
Koiliaris Agricultural	Koiliaris agricultural management – Green vegetable, Light Tilling
Clear Creek Natural	Clear Creek set aside
Clear Creek Agricultural	Clear Creek agricultural management – Corn and Soybeans, Tilling
Milia1	Milia terrace 1 - compost application for 10 years, every year
Milia2	Milia terrace 2 - compost application for 8 years, every year and then fallow for 2 years
Milia3	Milia terrace 3 - compost application for 10 years, every 3^{d} year
Damma Young	Young soils of Damma Glacier CZO - ages from 6 to 14 years old
Damma Intermediate	Intermediate soils of Damma Glacier CZO - ages from 57 to 79 years old
Damma Old	Old soils of Damma Glacier CZO - ages from 108 to 140 years old
Marchfeld Forest	Marchfeld forest development (0 - 400 years forest)
Marchfeld Grassland	Marchfeld land use conversion from forest to grassland (0 - 200 year forest – 200-400 year grassland)
Marchfeld Agricultural	Marchfeld land use conversion from forest to cropland (0 - 200 year forest – 200-400 year cropland)
Slavkov Forest	Slavkov Forest CZO - Forestry

710

711

Table 3: Comparison of the site data: SOC, Soil Characteristics and Meteorological data

	Soil characteristics			*SOC characteristics*		*Meteorological Data*		
Site	*Bulk Density* (gr/cm^3)	*Silt clay* (%)	*Clay* (%)	*DPM to RPM ratio*	*Initial SOC mass* (t C/ha-yr)	*Mean Temperature* (^oC)	*Mean Precipitation* (mm)	*Mean Pan Evaporation* (mm)
Heilongjiang Mollisols Alfa	1.35	77.6	42.0	0.25	13.77	2.5	510.6	514
Heilongjiang Mollisols NatF	‘’	‘’	‘’	0.15	‘’	‘’	‘’	‘’
Heilongjiang Mollisols F0C0	‘’	‘’	‘’	0.40	‘’	‘’	‘’	‘’
Heilongjiang Mollisols F1C0	‘’	‘’	‘’	1.00	‘’	‘’	‘’	‘’
Heilongjiang Mollisols F1C1	‘’	‘’	‘’	1.20	‘’	‘’	‘’	‘’
Heilongjiang Mollisols F1C2	‘’	‘’	‘’	1.44	‘’	‘’	‘’	‘’
Koiliaris CZO Natural	1.18	67.0	30.0	0.67	34.92	18.1	651.9	1916
Koiliaris CZO Agricultural	1.11	‘’	‘’	1.44	58.55	‘’	‘’	‘’
Milia 1	1.00	34.0	3.30	0.43	33.90	17.6	1494.6	1601.7
Milia 2	‘’	‘’	‘’	‘’	‘’	‘’	‘’	‘’
Milia 3	‘’	‘’	‘’	‘’	‘’	‘’	‘’	‘’
Clear Creek Natural	1.11	37.0	7.00	1.51	18.52	10.3	923.0	1413.6
Clear Creek Agricultural	‘’	‘’	‘’	2.00	32.38	‘’	‘’	‘’
Slavkov Forest CZO	1.30	47.0	11.00	0.25	55.36	5.3	1049.0	442.7
Marchfeld CZO Forest	2.00	73.6	16.36	0.25	20.00	9.1	687,0	727,7

Marchfeld CZO Grassland	1.26	‘’	‘’	0.70	27.11	‘’	‘’	‘’
Marchfeld CZO Cropland	1.26	‘’	‘’	1.44	‘’	‘’	‘’	‘’
Damma Glacier CZO Young Soils	1.50	35.0	3.10	1.44	0.60	4.0	1898.3	242.7
Damma Glacier CZO Intermediate Soils	1.50	‘’	‘’	‘’	1.05	2.9	‘’	‘’
Damma Glacier CZO Old soils	1.00	‘’	‘’	‘’	13.5	2.7	‘’	‘’

‘’ : The same value as the above cell

DPM = decomposable plant material

RPM = resistant plant material

712

713

Table 4: Description of the Calibration Parameters of the CAST model

Main CAST model calibration parameters		Description
Fragmentation	RPM to RPMc	Rate constant of fragmentation of Resistant Plant Material to coarse Resistant Plant Material
	RPMc to RPMf	Rate constant of fragmentation of coarse Resistant Plant Material to fine Resistant Plant Material
	RPMc(AC3) to RPMf(AC3)	Rate constant of fragmentation of coarse Resistant Plant Material to fine Resistant Plant Material within macro-aggregates
	DPMc(AC3) to DPMf(AC3)	Rate constant of fragmentation of coarse Decomposable Plant Material to fine Decomposable Plant Material within macro-aggregates
Macroaggregation	RPMc	Rate constant of coarse resistant plant material mass transfer for macro aggregate formation
	DPMc	Rate constant of coarse decomposable plant material mass transfer for macro aggregate formation
Microaggregation	RPMf(AC2inAC3)	Rate constant of fine resistant plant material mass transfer for micro aggregate formation within the macro aggregates
	DPMf(AC2inAC3)	Rate constant of fine decomposable plant material mass transfer for micro aggregate formation within the macro aggregates
Decomposition	fresh plant input(DPM)	Rate constant of decomposition of decomposable plant material from the plant litter pool
	BIO(AC1) within AC3	Rate constant of decomposition of Biomass carbon pools in Aggregate type 1 within Aggregate Type 3 ($AC1_{withinAC3}$)
	HUM(AC1) within AC3	Rate constant of decomposition of Humus in Aggregate type 1 within Aggregate Type 3 ($AC1_{withinAC3}$)
	BIO(AC2) within AC3	Rate constant of decomposition of Biomass carbon pools in Aggregate type 2 within Aggregate Type 3 ($AC2_{withinAC3}$)
	HUM(AC2) within AC3	Rate constant of decomposition of Humus in Aggregate type 2 within Aggregate Type 3 ($AC2_{withinAC3}$)

	BIO(AC2)	Rate constant of decomposition of Biomass carbon pools in Aggregate type 2
	HUM(AC2)	Rate constant of decomposition of Humus in Aggregate type 2
	BIO(AC1)	Rate constant of decomposition of Biomass carbon pools in Aggregate type 1
	HUM(AC1)	Rate constant of decomposition of Humus in Aggregate type 1
Contribution in macroaggregation	RPMc	Percent composition of macro aggregates (AC3) by coarse resistant plant material
	DPMc	Percent composition of macro aggregates (AC3) by coarse decomposable plant material
	AC1	Percent composition of macro aggregates (AC3) by silt clay sized aggregates (AC1)
	AC2	Percent composition of macro aggregates (AC3) by micro aggregates (AC2)
Contribution in microaggregation	RPMfwithin AC3	Percent composition of micro aggregates (AC2) by fine resistant plant material within macro aggregates (AC3)
	DPMfwithinAC3	Percent composition of micro aggregates (AC2) by fine decomposable plant material within macro aggregates (AC3)
	AC1within AC3	Percent composition of micro aggregates (AC2) by silt clay sized aggregates (AC1) within macro aggregates (AC3)
Disruption	DPM_f+DPM_c within AC3	fine and coarse DPM pool contents of the AC3 aggregate type, below which macro-aggregates are considered unstable
	DPM_f+DPM_c AC2 within AC3	fine and coarse DPM pool contents of the AC2 aggregate type within AC3 aggregate type, below which micro aggregates within macro aggregates are considered unstable
	DPM_f+DPM_c within AC2	fine and coarse DPM pool contents of the AC2 aggregate type, below which micro-aggregates are considered unstable

714

715

Table 5: Comparison of simulation results with regard to: Annual C stock and fluxes

Site	Simulation period (y)	Annual C Input (t C/ha/yr)			Annual C Storage (t C/ha/yr)			Annual CO_2 emissions (t C/ha/yr)			Bacterial Stock (BIO - t C/ha/yr)	
		Average	*min*	*max*	*Average*	*min*	*max*	*Average*	*min*	*max*	*Average*	*% of total stock*
Heilongjiang Mollisols - NatF	10	0.76	0.00	0.95	0.37	-0.61	1.12	0.33	0.08	0.49	8.00	4.49
Heilongjiang Mollisols - Alfa	‘’	0.94	‘’	1.17	0.47	‘’	1.31	0.41	0.11	0.57	8.35	4.52
Heilongjiang Mollisols - F0C0	‘’	0.69	‘’	0.86	0.26	-0.54	0.65	0.38	0.11	0.6	8.51	4.92
Heilongjiang Mollisols - F1C0	‘’	1.05	‘’	1.31	0.32	‘’	0.71	0.67	0.26	1.15	10.17	5.72
Heilongjiang Mollisols - F1C1	‘’	2.27	‘’	2.84	0.84	‘’	1.57	1.36	0.26	2.43	13.6	6.51
Heilongjiang Mollisols - F1C2	‘’	2.96	‘’	3.70	0.99	‘’	2.42	1.89	0.26	3.69	16.18	7.30
Koiliaris CZO Natural	100	3.80	3.80	3.80	0.48	-0.8	1.07	3.29	2.73	4.47	15.8	2.10
Koiliaris CZO Agricultural	40	0.36	0.36	0.36	-0.65	-2.34	-0.31	0.92	0.57	2.58	11.60	2.30
Milia 1	20	8.00	8.00	8.00	2.16	0.28	4.29	5.64	2.61	7.72	39.80	5.54
Milia 2	‘’	3.20	0.00	‘’	-0.21	-5.59	4.29	3.2	1.23	5.59	30.76	5.98
Milia 3	‘’	1.20	0.00	‘’	-0.65	-5.58	5.72	1.65	0.66	3.09	18.64	5.39

Clear Creek Natural	100	5.60	5.60	5.60	0.27	0.03	2.00	5.29	2.79	5.57	36.35	7.50
Clear Creek Agricultural	40	5.44	5.44	5.44	-0.42	-1.15	-0.12	5.35	5.07	6.19	7.90	3.08
Slavkov Forest CZO	20	2.75	2.75	2.75	0.72	-0.97	0.93	1.98	1.81	2.78	24.08	3.22
Marchfeld CZO Initial Forest	200	0.22	0.22	0.22	0.04	0.04	0.04	0.18	0.08	0.29	17.48	6.01
Marchfeld CZO Grassland	‘’	0.15	0.15	0.15	0.07	0.05	0.09	0.08	0.06	0.09	28.16	6.79
Marchfeld CZO Cropland	‘’	0.21	0.21	0.21	-0.04	-1.03	0.01	0.24	0.19	1.23	32.56	13.22
Damma Glacier CZO - Young Soils	14	0.07	0.07	0.07	0.03	0.02	0.03	0.04	0.02	0.04	3.86	36.56
Damma Glacier CZO - Intermediate Soils	44	0.72	0.10	1.80	0.31	0.03	0.82	0.4	0.04	1.11	4.72	12.40
Damma Glacier CZO - Old soils	40	1.12	0.20	2.00	0.24	-0.10	0.60	0.81	0.28	1.45	12.11	14.08

‘’: The same value as the above cell

Figures

Figure 1

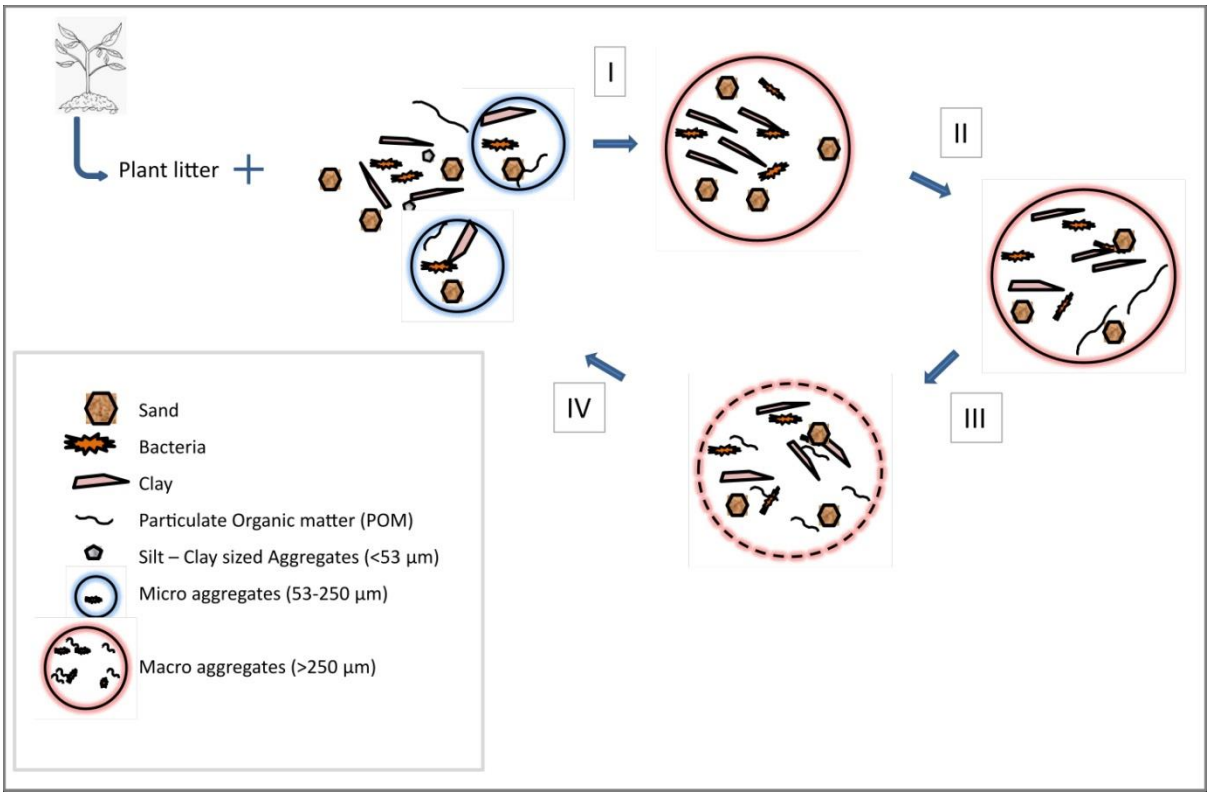

720 Figure 2

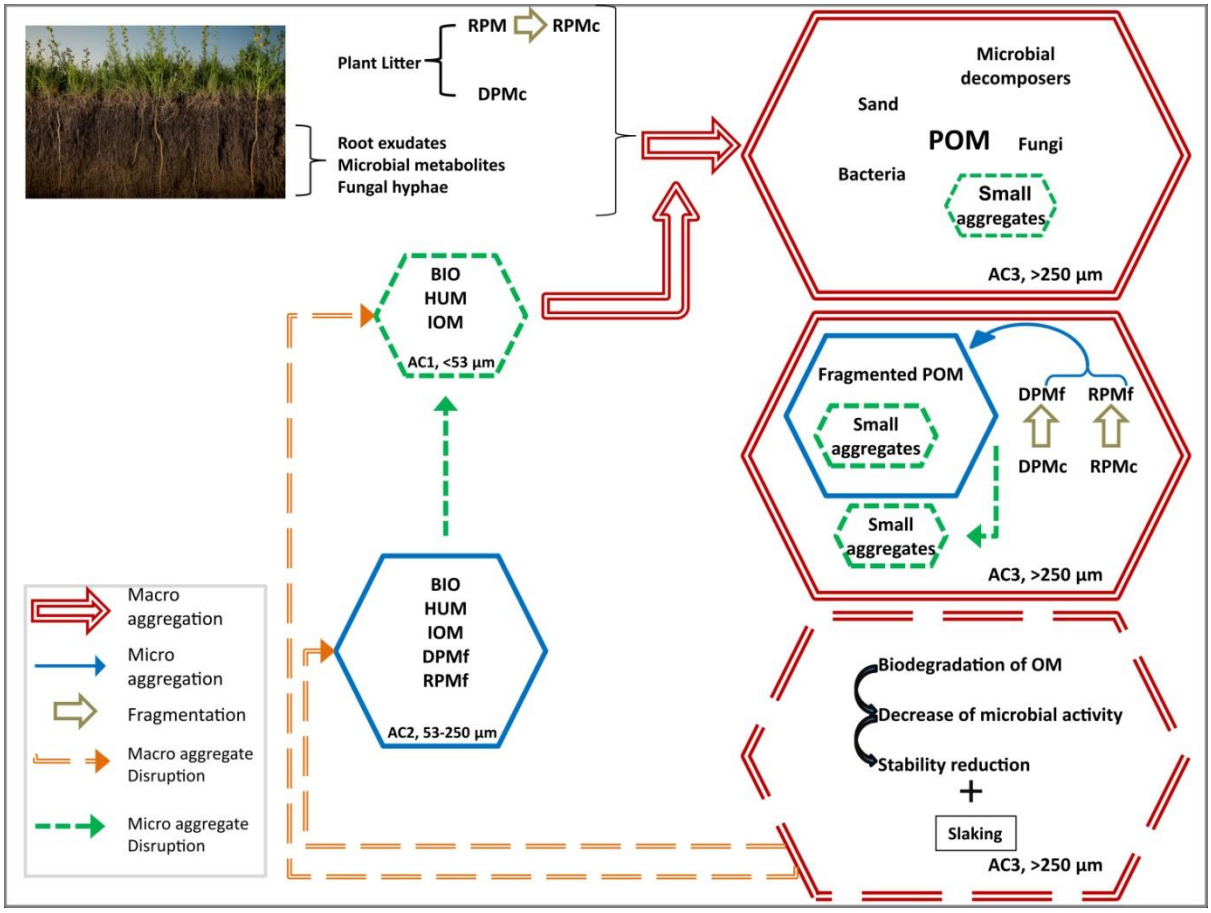

721

722 Figure 3

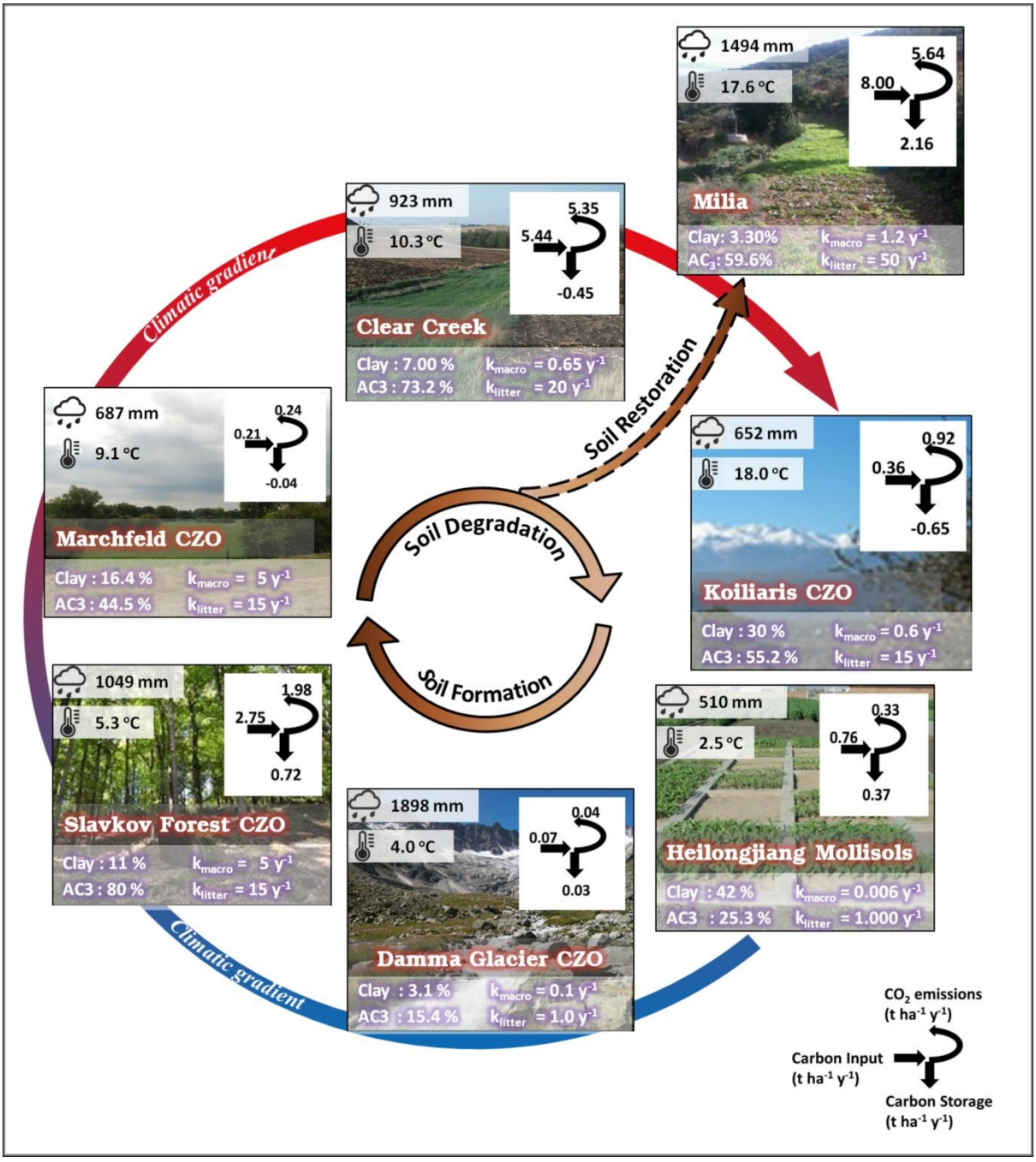

723

724 Figure 4

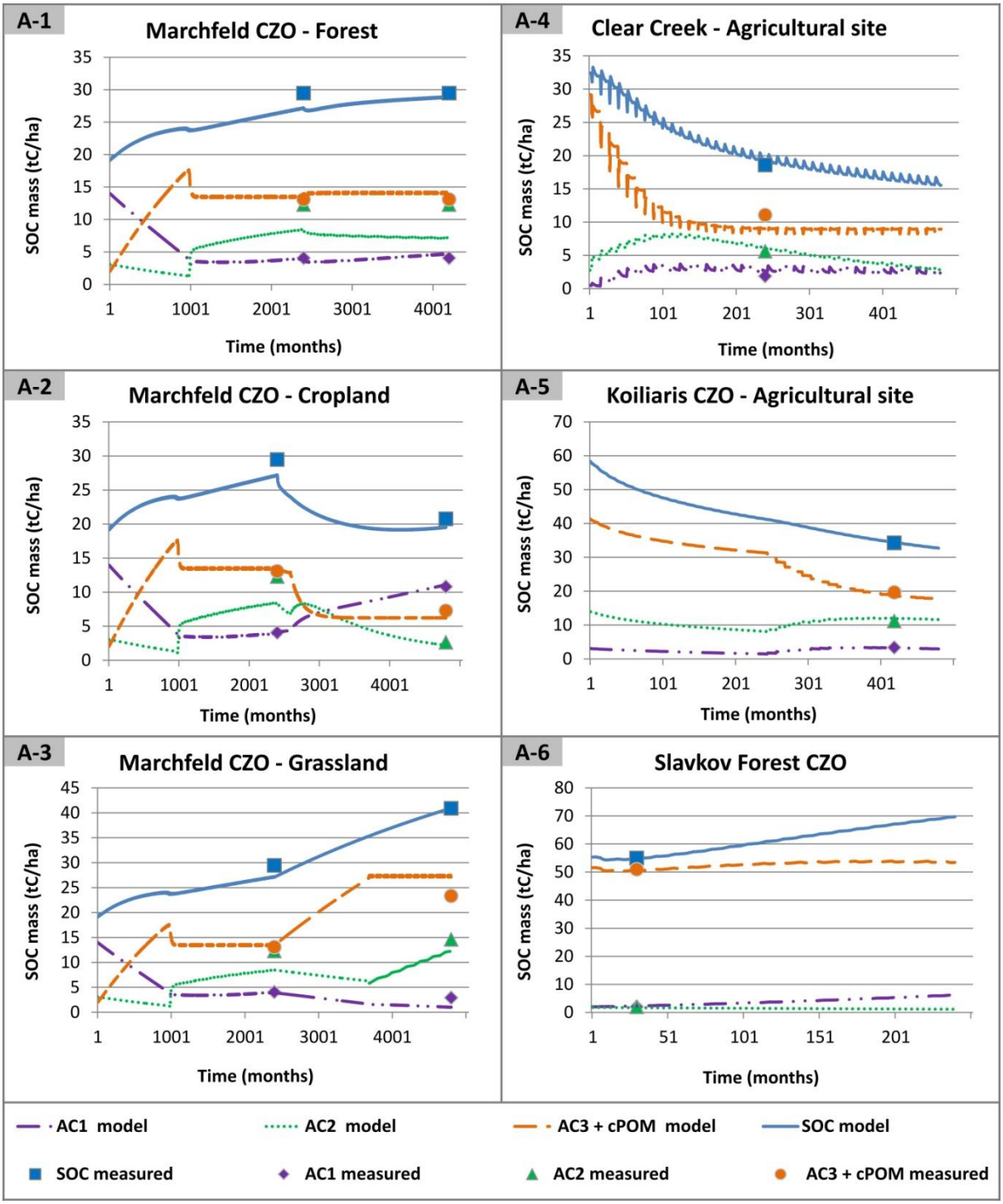

725

726 Figure 5a

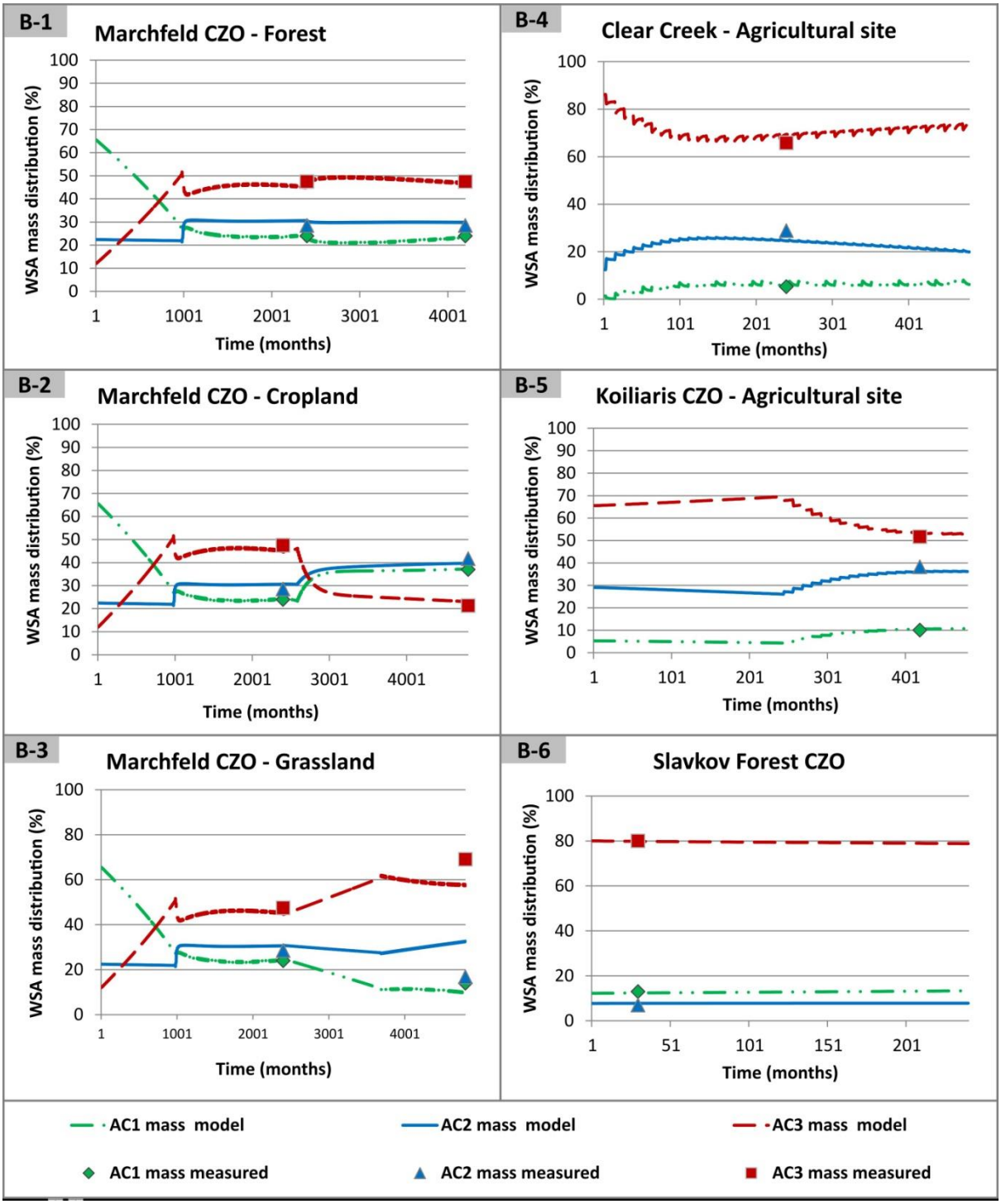
B-1
Marchfeld CZO - Forest
WSA mass distribution (%)
Time (months)
B-4
Clear Creek - Agricultural site
WSA mass distribution (%)
Time (months)
B-2
Marchfeld CZO - Cropland
WSA mass distribution (%)
Time (months)
B-5
Koiliaris CZO - Agricultural site
WSA mass distribution (%)
Time (months)
B-3
Marchfeld CZO - Grassland
WSA mass distribution (%)
Time (months)
B-6
Slavkov Forest CZO
WSA mass distribution (%)
Time (months)
AC1 mass model
AC2 mass model
AC3 mass model
AC1 mass measured
AC2 mass measured
AC3 mass measured

Figure 5b

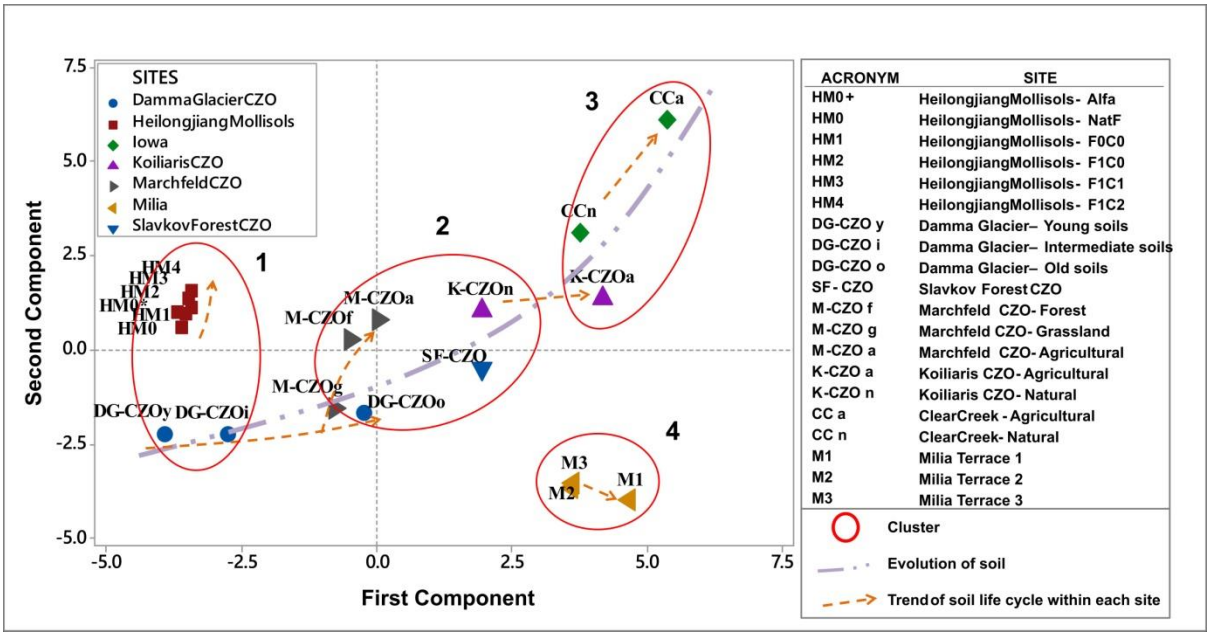

Figure 6

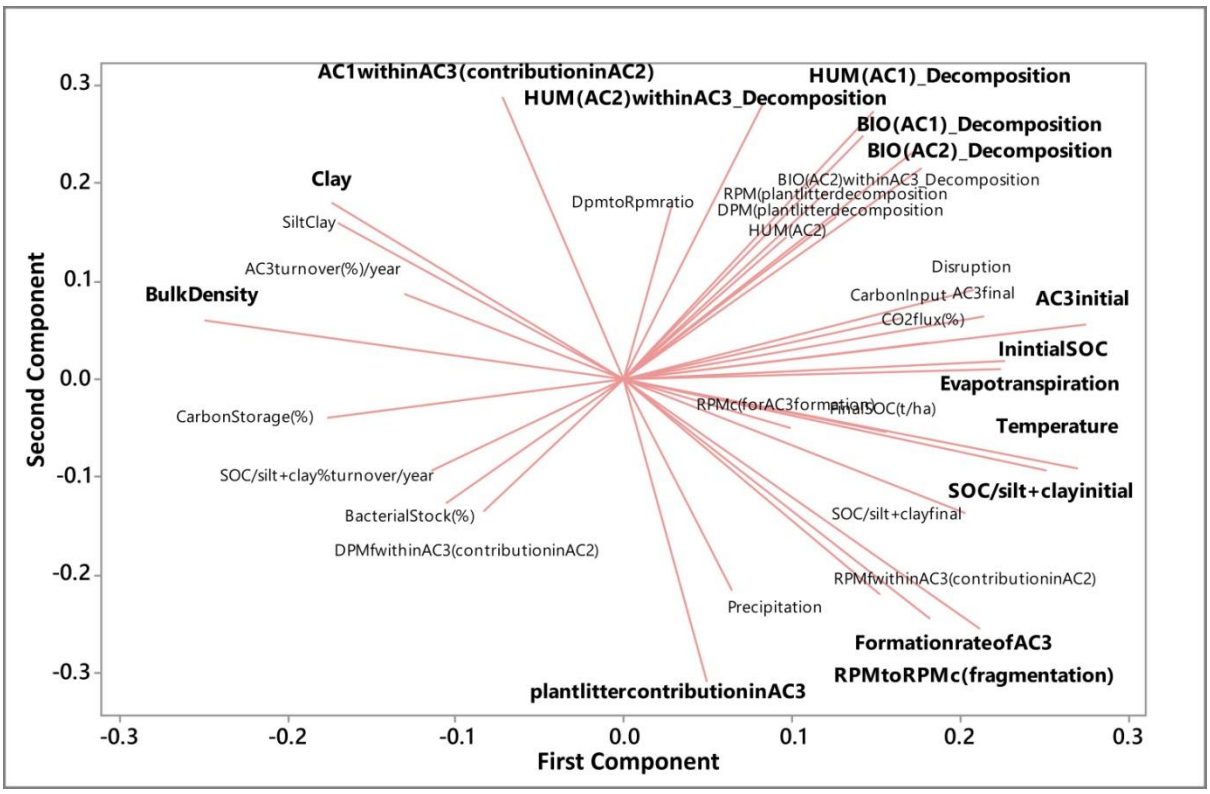

Figure 7

Figure Legends

Figure 1: Geographic distribution of the seven simulated sites (Google Earth, 2016)

Figure 2: Schematic representation of WSA formation modified from Stamati et al. (2013). The

particulate components that make up aggregates are not drawn to relative scale of their physical size.

Figure 3: Schematic representation of aggregation process, aggregate fractions and C pools included in the CAST model. The 3 large hexagons representing the AC1 macro-aggregate pool show in sequence, from top to bottom, 3 stages of macro-aggregate transformation from initial POM entering the soil, until it is decomposed resulting in breakup and release of AC2 and AC3 aggregate fractions.

Figure 4: Study sites placed on a temperature gradient representing different stages of soil evolution from soil formation to soil degradation, including soil restoration. The ordering of sites according to soil formation/degradation pathway also coincided with the temperature gradient.

Figure 5a: Calibration results of Koiliaris CZO (agricultural), Clear Creek (agricultural), Marchfeld CZO (all managements) and Slavkov Forest simulations for the SOC stock distribution together with the field (measured) data used for the calibration. Regarding the goodness of fit of the calibration of the model, the mean RMSE for the SOC is 0.55, which corresponds to 0.55 t C/ha for the SOC stock distribution in a range of 1.03 to 55 t C/ha

Figure 5b: Calibration results of Koiliaris CZO (agricultural), Clear Creek (agricultural), Marchfeld CZO (all managements) and Slavkov Forest simulations for the WSA distribution together with the field data used for the calibration. Regarding the goodness of fit of the calibration of the model, the mean RMSE for the WSA is 1.29

Figure 6: Score plot of the components PC1 and PC2 of the Principal Component Analysis

Figure 7: Loading Plot of the components PC1 and PC2 of the Principal Component Analysis